8

SPECTRAL DYNAMICS

In Chapter 6, the energy spectrum, defined as the Fourier transform of the autocorrelation, was introduced. There would be relatively little value in working with the spectrum, however, if it did not have its own physical interpretation. We shall find that spectral analysis allows us to draw conclusions that are almost unattainable in any other way. Spectra are decompositions of the measured function into waves of different periods or wavelengths. The value of the spectrum at a given frequency or wavelength is the mean energy in that wave, as we found in Section 6.4. Spectra thus give us an opportunity to think about the way in which waves, or eddies, of different sizes exchange energy with each other. This is the central issue in this chapter, because turbulence commonly receives its energy at large scales, while the viscous dissipation of energy occurs at very small scales. We shall find that there often exists a range of eddy sizes which are not directly affected by the energy maintenance and dissipation mechanisms; this range is called the inertial subrange.

8.1
One- and three-dimensional spectra

A turbulent flow varies randomly in all three space directions and in time. Experimental measurements, say of velocity, may be made along a straight line at a fixed time, at a fixed point as a function of time, or following a moving fluid point as a function of time. A measurement of this kind generates a random function of position or time. If the function is stationary or homogeneous, an autocorrelation can be formed and a spectrum can be computed. If the autocorrelation is a function of a time interval, the transform variable is a frequency; if the autocorrelation is a function of a spatial separation, the transform variable is a *wave number* (with dimensions length^{-1}). Spectra obtained in this way are called *one-dimensional spectra* because the measurements producing them were taken in one dimension.

Aliasing in one-dimensional spectra One-dimensional spectra do not seem very appropriate for the description of turbulence, because it is three dimensional. In a way, one-dimensional spectra give misleading information about three-dimensional fields. Suppose that we are making measurements along a straight line and that we are looking for components of wave number κ.

Because we are measuring along a line, we cannot distinguish between disturbances of wave number κ whose wave-number vector is aligned with the direction of measurement and disturbances of wave numbers larger than κ whose wave-number vector is oblique to the line of measurement (Figure 8.1). Thus, a one-dimensional spectrum obtained in a three-dimensional field contains at wave number κ contributions from components of all wave numbers larger than κ. This is called *aliasing*. Measured one-dimensional spectra ordinarily have a finite value at the origin (proportional to the integral scale). This does not mean that there is finite energy at zero wave number; the energy merely has been aliased from higher wave numbers to zero.

The problem of aliasing is not serious at high wave numbers, however. This is because small eddies tend to have about the same size in all directions, so that there is little chance that the situation depicted in Figure 8.1 occurs at small scales.

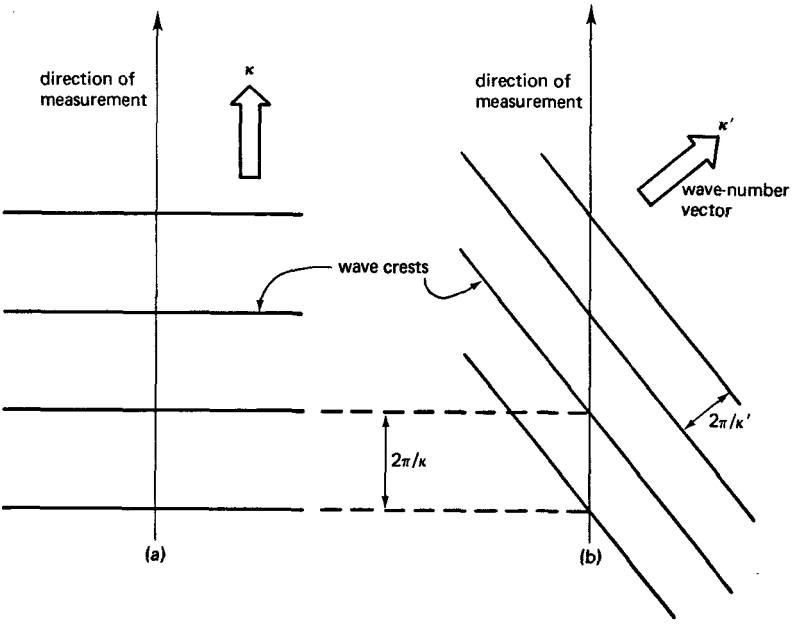

Figure 8.1. Aliasing in a one-dimensional spectrum: (a) a wave of true wave number κ, aligned with the line of measurement, (b) a wave of wave number $\kappa' > \kappa$, with wave-number vector oblique to the line of measurement.

The three-dimensional spectrum In order to avoid the aliasing problem, we can take measurements not just along a line but in all possible directions. This produces a correlation that is a function of the separation vector. The three-dimensional Fourier transform of such a correlation produces a spectrum that is a function of the wave-number vector κ_i. Unfortunately, this gives much more information than we can handle. The addition of the directional information eliminates the aliasing problem in exchange for a complexity that makes physical reasoning difficult. In order to remove the directional information, the spectrum is usually integrated over spherical shells around the origin of wave-number space. In this way, we obtain a spectrum that is a function of the scalar wave-number magnitude κ and whose value represents the total energy at that wave-number magnitude without aliasing. This is called a *three-dimensional spectrum.*

One additional problem remains. Often, the velocity components u_1, u_2, and u_3 are measured separately. However, for spectral analysis we need a spectrum that represents all of the kinetic energy at a given wave number. Therefore, the spectra of u_1, u_2, and u_3 are commonly added together; it is the spectrum of the total energy which is always referred to as the three-dimensional spectrum.

The correlation tensor and its Fourier transform Let us now formalize what we have described in words. The *correlation tensor* R_{ij} is defined by

$$R_{ij}(\mathbf{r}) \equiv \overline{u_i(\mathbf{x}, t)u_j(\mathbf{x} + \mathbf{r}, t)}. \tag{8.1.1}$$

The correlation tensor is a function of the vector separation $\mathbf{r}$ only, providing the turbulence is homogeneous. The spectrum tensor ϕ_{ij}, which is the Fourier transform of R_{ij}, is given by

$$\begin{aligned} \phi_{ij}(\boldsymbol{\kappa}) &= \frac{1}{(2\pi)^3} \int_{-\infty}^{\infty}\int\int\int \exp(-i\boldsymbol{\kappa} \cdot \mathbf{r})\, R_{ij}(\mathbf{r})\, d\mathbf{r}, \\ R_{ij}(\mathbf{r}) &= \int_{-\infty}^{\infty}\int\int\int \exp(i\boldsymbol{\kappa} \cdot \mathbf{r})\, \phi_{ij}(\boldsymbol{\kappa})\, d\boldsymbol{\kappa}. \end{aligned} \tag{8.1.2}$$

Unlike the definition of the spectrum used in Section 6.4, the correlation here has not been normalized; the form (8.1.2) is customary in the literature. Of primary interest is the sum of the diagonal components of ϕ_{ij}, which is

$\phi_{ii} = \phi_{11} + \phi_{22} + \phi_{33}$, because it represents the kinetic energy at a given wave-number vector. This becomes clear by considering $R_{ii}(0)$, which is

$$R_{ii}(0) = \overline{u_i u_i} = 3\mathscr{u}^2 = \int\int\int_{-\infty}^{\infty} \phi_{ii}(\boldsymbol{\kappa})\, d\boldsymbol{\kappa}. \tag{8.1.3}$$

The directional information in $\phi_{ii}(\boldsymbol{\kappa})$ is removed by integration over a spherical shell of radius κ (κ is the modulus of the vector $\boldsymbol{\kappa}$; that is, $\kappa^2 = \boldsymbol{\kappa}\cdot\boldsymbol{\kappa} = \kappa_i\kappa_i$). If we call the surface element of the shell $d\sigma$, we can write

$$E(\kappa) = \frac{1}{2} \oint\!\!\!\oint \phi_{ii}(\boldsymbol{\kappa})\, d\sigma. \tag{8.1.4}$$

The purpose of the factor $\frac{1}{2}$ is to make the integral of the three-dimensional spectrum $E(\kappa)$ equal to the kinetic energy per unit mass:

$$\int_0^\infty E(\kappa)\, d\kappa = \frac{1}{2}\int_0^\infty \left[\oint\!\!\!\oint \phi_{ii}(\boldsymbol{\kappa}) d\sigma\right] d\kappa = \frac{1}{2}\int\int\int_{-\infty}^{\infty} \phi_{ii}(\boldsymbol{\kappa})\, d\boldsymbol{\kappa}$$

$$= \tfrac{1}{2}\overline{u_i u_i} = \tfrac{3}{2}\mathscr{u}^2. \tag{8.1.5}$$

Two common one-dimensional spectra The one-dimensional spectra that are most often measured are the one-dimensional Fourier transforms of $R_{11}(r,0,0)$ and $R_{22}(r,0,0)$. The geometry involved in measuring R_{11} and R_{22} is sketched in Figure 8.2; $R_{11}(r,0,0)$ is called a *longitudinal correlation*, $R_{22}(r,0,0)$ is called a *transverse correlation*. Correspondingly, F_{11} is called a *longitudinal spectrum* and F_{22} is called a *transverse spectrum*.

The one-dimensional spectra $F_{11}(\kappa_1)$ and $F_{22}(\kappa_1)$ are defined by

$$R_{11}(r, 0, 0) \equiv \int_{-\infty}^{\infty} \exp(i\kappa_1 r)\, F_{11}(\kappa_1)\, d\kappa_1, \tag{8.1.6}$$

$$R_{22}(r, 0, 0) \equiv \int_{-\infty}^{\infty} \exp(i\kappa_1 r)\, F_{22}(\kappa_1)\, d\kappa_1. \tag{8.1.7}$$

The relations between F_{11}, F_{22}, and E are quite complicated. This can be seen by considering the relation between R_{11} and ϕ_{ij}, which is

$$R_{11}(r, 0, 0) = \int_{-\infty}^{\infty} \exp(i\kappa_1 r) \left(\int\int_{-\infty}^{\infty} \phi_{11}(\boldsymbol{\kappa})\, d\kappa_2\, d\kappa_3\right) d\kappa_1. \tag{8.1.8}$$

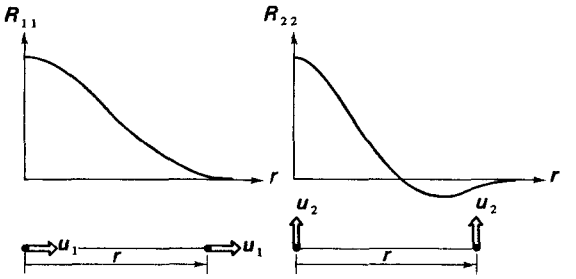

Figure 8.2. The longitudinal and transverse correlations.

Comparing (8.1.8) with (8.1.6), we find

$$F_{11}(\kappa_1) = \int_{-\infty}^{\infty}\int \phi_{11}(\boldsymbol{\kappa})\, d\kappa_2\, d\kappa_3. \tag{8.1.9}$$

This demonstrates the aliasing problem. The integration is over a slice of wave-number space at a given value of κ_1, so that energy from high wave numbers which are not located near the κ_1 axis is aliased to κ_1.

The shapes of F_{11} and F_{22} are somewhat different. Measured values of R_{11} do not ordinarily go negative (though there is no reason why they should not); this means that F_{11} has a maximum at the origin. Because F_{11} is majorized by its value at the origin, it curves downward parabolically away from $\kappa_1 = 0$ (note that F_{11} is symmetric because R_{11} is real).

The transverse correlation R_{22}, however, does become negative for some values of r (Figure 8.2). It is of interest to see why this occurs. Consider a plane perpendicular to the x_2 direction. Across this plane there should be no net mass flux, because the mean value of u_2 is zero. Therefore, the integral of u_2 over the entire x_1, x_3 plane should be zero:

$$\int_{-\infty}^{\infty}\int u_2(x_1, 0, x_3)\, dx_1\, dx_3 = 0. \tag{8.1.10}$$

If the integral is multiplied by u_2 at some given point, there results, after averaging,

$$\int_{-\infty}^{\infty}\int R_{22}(r_1, 0, r_3)\, dr_1\, dr_3 = 0. \tag{8.1.11}$$

This means that R_{22} must go negative somewhere in the x_1, x_3 plane. This

merely states that backflow is necessary somewhere in the plane in order to keep the net mass flux zero. If the turbulence is isotropic (meaning, as we saw in Chapter 3, that its statistics are invariant under reflections or rotations of the coordinate system), $R_{22}(r_1, 0, r_3)$ can be a function only of the distance $r = (r_1^2 + r_3^2)^{1/2}$. In this case, (8.1.11) becomes

$$\int_{-\infty}^{\infty} r R_{22}(r, 0, 0)\, dr = 0. \tag{8.1.12}$$

The transverse correlation thus must be negative somewhere. In Chapter 6 we found that the corresponding spectrum, F_{22}, is likely to have a peak away from the origin.

Experimental one-dimensional spectra are commonly obtained by moving a probe so rapidly through the turbulence that the velocity field does not change appreciably during the time of measurement. The probe sees a fluctuating velocity, which is a function of time; if the traversing speed U of the probe is large enough, the velocity signal $u(t)$ may be identified with $u(x/U)$. This approximation is known as *Taylor's hypothesis*; it is also referred to as the frozen-turbulence approximation. The substitution $t = x/U$ is a good approximation only if $u/U \ll 1$ (Hinze, 1959, Sec. 1.8; Lumley, 1965). This is an important constraint in the design of turbulence experiments.

Isotropic relations In general, the relations between F_{11}, F_{22}, and E are quite complicated. This is unfortunate; it seems natural to base physical reasoning on $E(\kappa)$, but most measurements give one-dimensional spectra like F_{11} and F_{22}. If the turbulence is isotropic, however, the relations between F_{11}, F_{22}, and E are fairly simple. The derivation of these isotropic relations is beyond the scope of this book. Two of the most useful relations are (Batchelor, 1953; Hinze, 1959)

$$E(\kappa) = \kappa^3 \frac{d}{d\kappa}\left(\frac{1}{\kappa}\frac{dF_{11}}{d\kappa}\right), \tag{8.1.13}$$

$$\frac{d}{d\kappa_1} F_{22}(\kappa_1) = -\frac{\kappa_1}{2}\frac{d^2}{d\kappa_1^2} F_{11}(\kappa_1). \tag{8.1.14}$$

The first of these is often used to obtain E from measured values of F_{11} at high wave numbers. This procedure is legitimate because turbulence is very nearly isotropic at high wave numbers.

According to (8.1.13) and (8.1.14), $F_{11} \propto \kappa_1^n$ and $F_{22} \propto \kappa_1^n$ if $E \propto \kappa^n$. The

exponent in the power law is the same, but the coefficients are different. We shall find shortly that in a major part of the spectrum $E \propto \kappa^{-5/3}$; it is encouraging to know that F_{11} and F_{22} exhibit the same power law. If all spectra are proportional to $\kappa^{-5/3}$, (8.1.14) gives $F_{22} = \frac{4}{3}F_{11}$. This relation is often used to examine turbulence for evidence of isotropy.

The isotropic relations also give some indication of the shapes of F_{11}, F_{22}, and E near the origin. Because R_{11} is real and positive (no experiments are known in which $R_{11} < 0$ anywhere), F_{11} is symmetric and majorized by its value at the origin:

$$F_{11}(\kappa) = A_1 - B\kappa_1^2 + C\kappa_1^4 + \dots . \tag{8.1.15}$$

Substituting this into (8.1.13, 8.1.14), we obtain

$$E(\kappa) = 8C\kappa^4 + \dots , \tag{8.1.16}$$

$$F_{22}(\kappa_1) = A_2 + \tfrac{1}{2}B\kappa_1^2 + \dots . \tag{8.1.17}$$

Thus, E begins from zero, quartically upward, while F_{22} curves upward parabolically, so that it has a peak away from the origin. The quartic behavior of $E(\kappa)$ deserves special attention. Physically, the point is that there is no energy at zero wave number, so that $\phi_{ii}(0) = 0$. Because ϕ_{ii} is symmetric, it begins parabolically ($\propto \kappa^2$). Now, $E(\kappa)$ is an integral of ϕ_{ii} over a spherical shell whose area is proportional to κ^2, so that $E(\kappa)$ must be proportional to κ^4 near the origin. A much more careful analysis is needed to show that this result is not restricted to isotropic turbulence. Also, the coefficient in the parabolic form of ϕ_{ii} near the origin is not the same in all directions, but that has no effect on the behavior of E (Lumley, 1970). It should be kept in mind, however, that the large-scale structure of turbulence is unlikely to be isotropic, so that (8.1.13) and (8.1.14) should not be used to obtain quantitative results at small wave numbers.

Spectra of isotropic simple waves We may get an impression of the shapes of one- and three-dimensional spectra by examining a rather artificial case. Consider an isotropic field of waves that all have the same wavelength $2\pi/\kappa_*$, but whose wave-number vectors have random directions. For this isotropic field, ϕ_{ii} is zero, except on a shell of radius κ_*, where it has a uniform distribution. Therefore, $E(\kappa)$ is zero everywhere, except for a spike at $\kappa = \kappa_*$. The shape of F_{11} can be computed from (8.1.9). If the plane of integration is beyond κ_*, F_{11} is zero; if $\kappa_1 \leqslant \kappa_*$, the integration yields

$$F_{11}(\kappa_1) = \frac{A}{2\kappa_*^3}(\kappa_*^2 - \kappa_1^2). \tag{8.1.18}$$

Here, A is an arbitrary constant, related to the area under the spike in $E(\kappa)$. Substitution of (8.1.18) into (8.1.14) gives an expression for F_{22}; again, $F_{22} = 0$ for $\kappa_1 > \kappa_*$, while for $\kappa_1 \leqslant \kappa_*$

$$F_{22}(\kappa_1) = \frac{A}{4\kappa_*^2}(\kappa_*^2 + \kappa_1^2). \tag{8.1.19}$$

These spectra are shown in Figure 8.3a. It should be noted that F_{11} curves parabolically downward, while F_{22} curves upward.

In a general isotropic field, $E(\kappa)$ can be thought of as being made up from spikes of different amplitudes at different wave numbers, so that F_{11} and

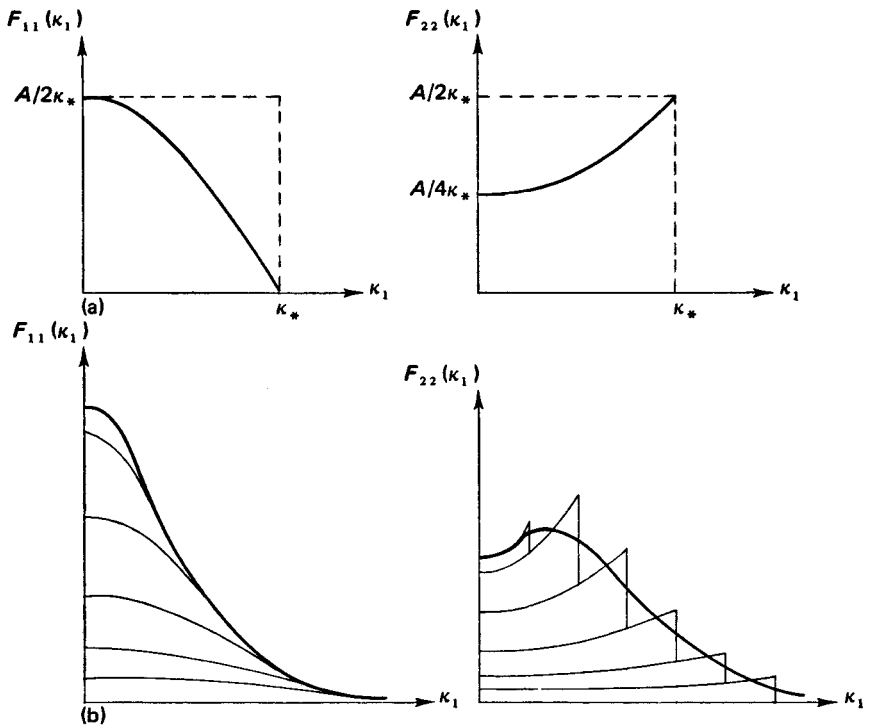

Figure 8.3. Longitudinal and transverse spectra of fields of isotropic simple waves: (a) spectra for a field of simple waves of wave number κ_*, (b) composite spectra for a field of waves with different wave numbers (adapted from Corrsin, 1959).

F_{22} can be constructed by adding many spectra of the type sketched in Figure 8.3a. It is evident that the longitudinal spectrum is likely to be a monotone decreasing function, while the transverse spectrum is likely to rise at first before it decreases (Figure 8.3b). Of course, both spectra should go to zero as $\kappa_1 \to \infty$, because the total area under the curves is proportional to the kinetic energy.

8.2
The energy cascade

The existence of energy transfer from large eddies to small eddies, driven by vortex stretching and leading to viscous dissipation of energy near the Kolmogorov microscale, was demonstrated in Chapter 3. Here, we discuss how the energy exchange takes place.

Let us briefly recall the vortex-stretching mechanism. When vorticity finds itself in a strain-rate field, it is subject to stretching. On the basis of conservation of angular momentum, we expect that the vorticity in the direction of a positive strain rate is amplified, while the vorticity in the direction of a negative strain rate is attenuated. This effect is sketched in Figure 8.4. If the influence of viscosity is ignored, the vorticity equation reads (recall that s_{ij} is the strain-rate tensor)

$$d\omega_i/dt = \omega_j s_{ij}. \tag{8.2.1}$$

Consider the two-dimensional strain-rate field in Figure 8.4. Here, $s_{11} = -s_{22} = s$, while $s_{12} = 0$. Let us assume that s is a constant for all $t > 0$ and that $\omega_1 = \omega_2 = \omega_0$ at $t = 0$. In this case, (8.2.1) reduces to

$$d\omega_1/dt = s\omega_1, \quad d\omega_2/dt = -s\omega_2. \tag{8.2.2}$$

This yields

$$\omega_1 = \omega_0 e^{st}, \quad \omega_2 = \omega_0 e^{-st}, \tag{8.2.3}$$

$$\omega_1^2 + \omega_2^2 = 2\omega_0^2 \cosh 2st. \tag{8.2.4}$$

Except for very small values of st, the total amount of vorticity thus increases with increasing values of st. The vorticity component in the direction of stretching increases rapidly, while the vorticity component in the direction of compression (shrinking) decreases slowly at large st. This is similar to the rate of growth of a spot of contaminant (Section 7.3); of course, the same stretch-

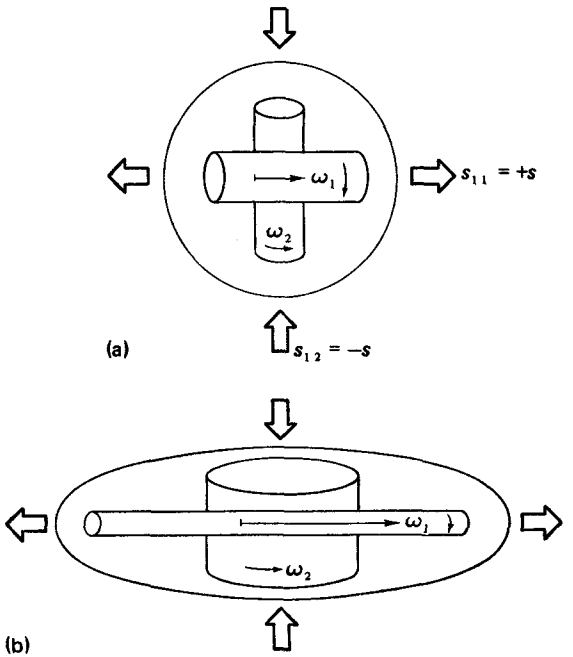

Figure 8.4. Vorticity stretching in a strain-rate field: (a) before stretching, (b) after stretching.

ing mechanism is involved. Note, however, that viscous effects are not accounted for in (8.2.1, 8.2.2).

Vortex stretching involves an exchange of energy, because the strain rate performs deformation work on the vortices that are being stretched. We learned in Chapter 3 that the amount of energy gained by a disturbance with velocity components u_i, u_j in a strain rate s_{ij} is equal to $-u_i\, u_j\, s_{ij}$ per unit mass and time. In the plane strain-rate field of Figure 8.4, the energy exchange rate is

$$T = s(u_2^2 - u_1^2). \tag{8.2.5}$$

Now, the vorticity component ω_1 is increased, which corresponds to an increase in u_2 and u_3; also, ω_2 is decreased, which corresponds to a decrease in u_1 and u_3. We thus expect that u_2^2 increases and u_1^2 decreases, while u_3^2 increases fairly slowly. Hence, the difference $u_2^2 - u_1^2$, although starting from zero at $t = 0$, becomes positive. This means that T also becomes positive, so

that the strain rate indeed performs work on the eddies in Figure 8.4. The total amount of energy in the vortices is thus expected to increase.

Spectral energy transfer A turbulent flow field can (conceptually, at any rate) be imagined as divided into all eddies smaller than a given size and all eddies larger than that size. The smaller eddies are exposed to the strain-rate field of the larger eddies. Because of the straining, the vorticity of the smaller eddies increases, with a consequent increase in their energy at the expense of the energy of the larger eddies. In this way, there is a flux of energy from larger to smaller eddies.

The situation is not yet quite clear, however. Although we expect that there will be a net flux of energy from smaller to larger wave numbers, we do not know which eddy sizes are involved in the spectral energy transfer across a given wave number. For example, does the energy come from eddies that are slightly larger than a given wavelength, or does it come from all larger eddies indiscriminately? In the same way, is the energy absorbed at wave numbers slightly larger than a given value, or is it absorbed by all larger wave numbers? We attempt to answer these questions by looking at the characteristic strain rates of different eddy sizes. Before we do this, however, we need a better mental picture of the concept of an eddy.

A simple eddy Let us recall that an autocorrelation and the corresponding spectrum are a Fourier-transform pair. If the correlation is a function of spatial separation, the spectrum is a function of wave number. A certain eddy size, say ℓ, is thus associated with a certain wave number, say κ. An "eddy" of wave number κ may be thought of as some disturbance containing energy in the vicinity of κ. It would be tempting to think of an eddy as a disturbance contributing a narrow spike to the spectrum at κ. However, a narrow spike in the spectrum creates slowly damped oscillations (of wavelength $2\pi/\kappa$) in the correlation, as we discovered in Section 6.2. Such a correlation is characteristic of wavelike disturbances, but not of eddies; we expect eddies to lose their identity because of interactions with others within one or two periods or wavelengths. Therefore, the contribution of an eddy to the spectrum should be a fairly broad spike, wide enough to avoid oscillatory behavior ("ringing") in the correlation.

It is convenient to define an eddy of wave number κ as a disturbance containing energy between, say 0.62κ and 1.62κ. This choice centers the

energy around κ on a logarithmic scale, because $\ln(1.62) = \ln(1/0.62) \cong \frac{1}{2}$; it also makes the width of the contribution to the spectrum equal to κ (Figure 8.5). We recall from Section 6.2 that the transform of a narrow band around κ is a wave of wavelength $2\pi/\kappa$, with an envelope whose width is the inverse of the bandwidth. Now, because the bandwidth selected is κ, the width of the envelope of the eddy is of order $1/\kappa$. This is sketched in Figure 8.5; we see that an eddy defined this way is indeed the relatively compact disturbance we want it to be. The eddy size ℓ is roughly equal to $2\pi/\kappa$.

The schematic eddy presented in Figure 8.5 suffices for the development of energy-cascade concepts. This model, however, cannot deal with all of the problems associated with the distinction between waves and eddies. The Fourier transform of a velocity field is a decomposition into waves of different wavelengths; each wave is associated with a single Fourier coefficient. An eddy, however, is associated with many Fourier coefficients and the phase relations among them. Fourier transforms are used because they are convenient (spectra can be measured easily); more sophisticated transforms are needed if one wants to decompose a velocity field into eddies instead of waves (Lumley, 1970).

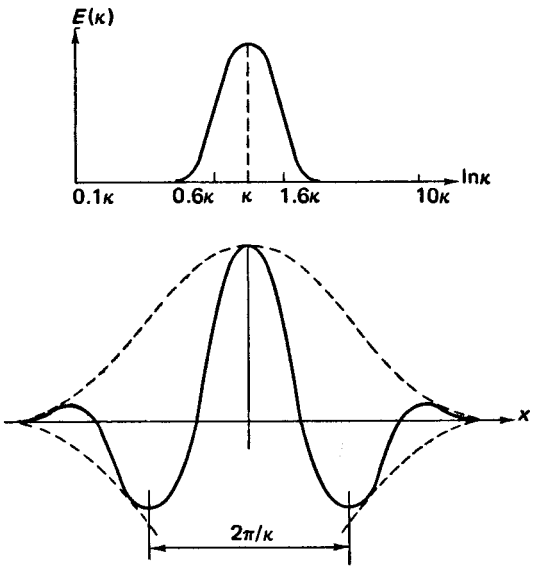

Figure 8.5. An eddy of wave number κ and wavelength $2\pi/\kappa$.

The energy cascade Let us return to the role of the strain rates of different eddy sizes in the spectral energy exchange mechanism. The energy of all eddies of size $2\pi/\kappa$ is roughly proportional to $E(\kappa)$ times the width of the eddy spectrum, which is κ. Hence, a characteristic velocity is given by $[\kappa E(\kappa)]^{1/2}$. The size of the eddy is about $2\pi/\kappa$, so that the characteristic strain rate (and the characteristic vorticity) of an eddy of wave number κ is given by

$$s(\kappa) = \frac{(\kappa E)^{1/2}}{2\pi/\kappa} = \frac{(\kappa^3 E)^{1/2}}{2\pi}. \tag{8.2.6}$$

We recall from Section 3.2 that the strain rate of large eddies, which contain most of the energy, is of order u/ℓ (ℓ is an integral scale), while the small-scale strain-rate fluctuations are of order u/λ (λ is a Taylor microscale). Therefore, we should expect that the strain rate $s(\kappa)$ increases with wave number. We find in the next section that $E(\kappa) \propto \kappa^{-5/3}$ in the central part of the spectrum; this gives $s(\kappa) \propto \kappa^{2/3}$, so that $s(\kappa)$ indeed increases with κ. We shall use this result for convenience.

The energy spectrum is continuous; for the purposes of this discussion, however, we may think of the spectrum as being made up from eddies of discrete sizes. The strain rate imposed on eddies of wave number κ due to the eddies of the next larger size (which extends from 0.24κ to 0.62κ, centered around 0.38κ) is $s(0.38\kappa)$, which is about $\frac{1}{2}s(\kappa)$ if $s(\kappa) \propto \kappa^{2/3}$. The strain rate due to eddies two sizes larger than $2\pi/\kappa$ (whose energy extends from 0.09κ to 0.24κ, centered around 0.15κ) is again about half as large. Adding all of the strain rates of eddies larger than $2\pi/\kappa$, we conclude that of the total strain rate felt by an eddy of wave number κ, one-half comes from eddies of the next larger size, and another quarter from the next larger size. Therefore, we expect that most of the energy crossing a given wave number comes from eddies with slightly smaller wave numbers.

The question now is which eddies benefit most from the energy transfer across wave number κ. According to (8.2.5), energy transfer depends upon the ability of the strain rate to align the smaller eddies so that u_2^2 and u_1^2 (of the eddies in Figure 8.4) become different. The strain rate thus has to overcome the tendency of eddies to equalize u_1^2, u_2^2, and u_3^2. This tendency is called *return to isotropy*; the lack of isotropy (or anisotropy) that can be generated by the strain rate depends on the time scale for return to isotropy

relative to the time scale of the straining motion. Because the strain rate has dimensions of time^{-1}, the time scale of return to isotropy is roughly $1/s(\kappa)$ for eddies of wave number κ. This means that those eddies would return to isotropy in a time of order $1/s(\kappa)$ if the strain rate were removed. Because smaller eddies have larger strain rates, small eddies return to isotropy rapidly.

If $\mathscr{S}$ is the combined strain rate of all eddies with wave numbers below κ, the time scale of the applied strain rate is of order $1/\mathscr{S}$. If $\mathscr{S}$ is large compared to $s(\kappa)$, the anisotropy is large; if $\mathscr{S}$ is small compared to $s(\kappa)$, the relatively rapid return to isotropy prevents the creation of a large anisotropy. It appears reasonable to assume that the degree of anisotropy is proportional to $\mathscr{S}/s(\kappa)$. The energy transferred from all larger eddies to an eddy of wave number κ is then approximately $\mathscr{S}^2\kappa E(\kappa)/s(\kappa)$, by virtue of (8.2.5). The energy absorbed by eddies of the next smaller size (with energy between 1.6κ and 4.2κ, centered around 2.6κ) is about $\frac{1}{4}\mathscr{S}^2\kappa E(\kappa)/s(\kappa)$, because $s(2.6\kappa) \cong 2s(\kappa)$ and $2.6\kappa E(2.6\kappa) \cong \frac{1}{2}\kappa E(\kappa)$ if $E(\kappa) \propto \kappa^{-5/3}$. Eddies of wave number κ thus receive about two-thirds of the total energy transfer, those of the next smaller size receive about one-sixth, and all smaller eddies combined also receive about one-sixth.

A crude picture is beginning to emerge. Most of the energy that is exchanged across a given wave number apparently comes from the next larger eddies and goes to the next smaller eddies. It seems fair to describe the energy transfer as a cascade, much like a series of waterfalls, each one filling a pool that overflows into the next one below. This concept proves to be exceptionally useful, because the largest eddies and the smallest eddies clearly have no direct effect on the energy transfer at intermediate wave numbers. However, we should not expect too much from the cascade model. After all, it is a very leaky cascade if half the water crossing a given level comes directly from all other pools uphill.

In the development of the cascade model, a number of crude assumptions have been made, some of which are not likely to be valid throughout the spectrum. One major assumption is clearly not valid at very small scales. The time scale of an eddy has been estimated as $1/s(\kappa)$; however, there is a viscous lower limit on time scales, as we saw in Chapters 1 and 3. The smallest time scale is $(\nu/\epsilon)^{1/2}$ and the strain rate of very small eddies is of order $(\epsilon/\nu)^{1/2}$, so that the model developed here is not valid if $s(\kappa)$ and $(\epsilon/\nu)^{1/2}$ become of the same order of magnitude. The cascade model is inviscid; it should be applied only to eddy sizes whose Reynolds number $s(\kappa)/\kappa^2\nu$ is large.

8.3
The spectrum of turbulence

We have found that the anisotropy of eddies depends on the time-scale ratio $\mathscr{S}/s(\kappa)$. The strain rate of the large, or "energy-containing" eddies is comparable to the strain rate of the mean flow (recall that $\partial U/\partial y \sim u/\ell$). Therefore, large eddies have a steady anisotropy due to the strain rate of the mean flow, which maintains a steady orientation. On the other hand, the strain rate of small eddies is large compared to that of the mean flow and of the large eddies (recall that $s_{ij} \sim u/\lambda$), so that no permanent anisotropy can be induced at small scales. This does not mean that small eddies are isotropic, because energy transfer is possible only if eddies are aligned with a strain rate. However, the anisotropy discussed in the preceding section is temporary; eddies of a given size are stretched mainly by somewhat larger eddies, whose strain-rate field is constantly shifting in magnitude and direction. As the eddy size becomes smaller, the permanent isotropy decreases, so that at small scales the strain-rate field itself may be expected to be isotropic in the mean. In other words, turbulence is increasingly "scrambled" at small scales, and any permanent sense of direction is lost. This concept is called *local isotropy*; it was proposed by A. N. Kolmogorov in 1941 (see Friedlander and Topper, 1962). The adjective "local" refers to small scales (large wave numbers).

Local isotropy does not exist if the Reynolds number is not large enough. The strain rate of the mean flow is of order u/ℓ, the strain rate of the smallest eddies is of order $u/\lambda \sim (\epsilon/\nu)^{1/2}$. We probably need $u/\lambda \geqslant 10u/\ell$ in order to have local isotropy at the smallest scales. Consequently, $\ell/\lambda \sim R_\ell^{1/2}$ (3.2.17) needs to be at least 10, giving a Reynolds number of at least 100.

In the part of the spectrum in which local isotropy prevails, time scales are short compared to those of the mean flow. This means that small eddies respond quickly to changing conditions in the mean flow. Therefore, small eddies always are in approximate equilibrium with local conditions in the mean flow, even though the latter may be evolving. For this reason, the range of wave numbers exhibiting local isotropy is called the *equilibrium range*. It begins at a wave number where $s(\kappa)$ first becomes large compared to the mean strain rate, and it includes all higher wave numbers.

The spectrum in the equilibrium range In the equilibrium range, time scales are so short that the details of the energy transfer between the mean flow and the turbulence (which occurs mainly at large scales) cannot be important.

However, the amount of energy cascading down the spectrum should be a major parameter. Because all energy is finally dissipated by viscosity, the total amount of energy transfer must be equal to the dissipation rate ϵ, and the second major parameter should be the viscosity itself. If no other parameters are involved, we have $E = E(\kappa,\epsilon,\nu)$, which can have only one nondimensional form:

$$\frac{E(\kappa)}{\nu^{5/4}\epsilon^{1/4}} = \frac{E(\kappa)}{v^2\eta} = f(\kappa\eta). \tag{8.3.1}$$

This scaling law was derived by Kolmogorov; as before, $\eta = (\nu^3/\epsilon)^{1/4}$ is the Kolmogorov microscale and $v = (\nu\epsilon)^{1/4}$ is the Kolmogorov velocity. The Kolmogorov spectrum (8.3.1) is supported by a large amount of experimental data. Because the turbulence in the equilibrium range is isotropic, the isotropic relations (8.1.13, 8.1.14) may be used to compute E and F_{22} from measured F_{11}.

The similarity between (8.3.1) and the law of the wall in turbulent boundary layers (Chapter 5) is striking. Close to a rigid wall, the momentum flux is ρu_*^2; if u_*^2 and ν are the only parameters, $U = U(y,u_*^2,\nu)$, so that $U/u_* = f(yu_*/\nu)$. In boundary layers, the spatial momentum flux is involved; in the spectrum, it is the spectral energy flux..

Most of the viscous dissipation of energy occurs near the Kolmogorov microscale η, as we discussed in Chapter 3. The equilibrium range thus includes the *dissipation range* of wave numbers, much like the wall layer of a boundary layer includes the viscous sublayer (Section 5.2). It can be shown that the spectrum of the dissipation, $D(\kappa)$, is given by (Batchelor, 1953; Hinze, 1959)

$$D(\kappa) = 2\nu\kappa^2 E(\kappa). \tag{8.3.2}$$

The dissipation is proportional to the square of velocity gradients; the factor κ^2 in (8.3.2) arises because differentiation corresponds to multiplication by wave number. The dissipation rate ϵ is given by

$$\epsilon = 2\nu\overline{s_{ij}s_{ij}} = \int_0^\infty D(\kappa)\,d\kappa = 2\nu\int_0^\infty \kappa^2 E\,d\kappa. \tag{8.3.3}$$

If most of the dissipation occurs within the equilibrium range, we obtain, with (8.3.1),

$$\int_0^\infty (\kappa\eta)^2 f(\kappa\eta)\,d(\kappa\eta) = \tfrac{1}{2}. \tag{8.3.4}$$

The value of ϵ often is determined by integrating (8.3.3) with a measured energy spectrum.

The large-scale spectrum For small wave numbers, the spectrum scales in a different way. If the spectral Reynolds number $s(\kappa)/\kappa^2\nu$ is large, we do not expect viscosity to be relevant. The principal parameters are those that describe the energy transfer from the mean flow to the turbulence and the energy transfer from large to small scales. The turbulence receives its energy from the mean strain rate S and transfers energy to small scales at a rate ϵ, so that the scaling of the large-scale part of the spectrum should be based on S and ϵ. If these are the only relevant parameters, we must have $E = E(\kappa,\epsilon,S)$. For convenience, we define S and ℓ by the relations $S \equiv u/\ell$ and $\epsilon \equiv u^3/\ell$. The spectrum then becomes

$$\frac{E(\kappa)}{\epsilon^{3/2}S^{-5/2}} = \frac{E(\kappa)}{u^2\ell} = F(\kappa\ell). \tag{8.3.5}$$

This relation, of course, is not universal, but differs in flows with different geometries. In a family of flows with the same geometry, however, we expect the large-scale part of the spectrum to scale like (8.3.5).

The inertial subrange The Kolmogorov spectrum (8.3.1) is related to a limit process in which $s(\kappa)/S \to \infty$. Evaluating $s(\kappa)$ with (8.2.6) and (8.3.1), we find that this limit corresponds to

$$\frac{s(\kappa)}{S} = \frac{R_\ell^{1/2}}{2\pi}\,[(\kappa\eta)^3 f(\kappa\eta)]^{1/2} \to \infty. \tag{8.3.6}$$

Here we used $S = u/\ell$ and $R_\ell = u\ell/\nu$. It is clear that the Kolmogorov spectrum is valid for $\kappa\eta = \mathcal{O}(1)$ in the limit as $R_\ell \to \infty$. On the other hand, the large-scale spectrum (8.3.5) applies to wave numbers for which $s(\kappa)/\kappa^2\nu \to \infty$. With (8.2.6) and (8.3.5), this limit becomes

$$\frac{s(\kappa)}{\kappa^2\nu} = \frac{R_\ell}{2\pi}\,[(\kappa\ell)^{-1} F(\kappa\ell)]^{1/2} \to \infty. \tag{8.3.7}$$

This implies that (8.3.5) is valid for $\kappa\ell = \mathcal{O}(1)$ and $R_\ell \to \infty$. We thus have viscous scaling at high wave numbers and inertial scaling at low wave numbers, both valid in the limit as $R_\ell \to \infty$. This is similar to the scaling laws for channel flow (Section 5.2), where we used an inviscid description for

$y/h = \mathcal{O}(1)$ and a viscous description for $yu_*/\nu = \mathcal{O}(1)$, both in the limit as $R_* \to \infty$. We found that those scaling laws had a common region of validity; perhaps we can do the same here.

The existence of a region of "overlap" depends on the possibility of taking the limits $\kappa\eta \to 0$ and $\kappa\ell \to \infty$ simultaneously. In other words, we should be able to go to the small-scale end of the large-scale spectrum and to the large-scale end of the Kolmogorov spectrum simultaneously, without violating the condition $R_\ell \to \infty$ required by (8.3.6, 8.3.7). Take $\kappa\ell = R_\ell^n$ $(n > 0)$ and recall that $\ell/\eta \sim R_\ell^{3/4}$ (1.5.14). We obtain

$$\kappa\eta = \kappa\ell(\eta/\ell) \sim \kappa\,\ell R_\ell^{-3/4} = R_\ell^{n-3/4}, \tag{8.3.8}$$

so that we need $0 < n < 3/4$ in order to obtain $\kappa\eta \to 0$. Because we do not know how $f(\kappa\eta)$ and $F(\kappa\ell)$ vary, we cannot tell if (8.3.6) and (8.3.7) will indeed be satisfied. We assume that they are, though, and verify the conditions after the matching has been performed.

With $0 < n < 3/4$, it is possible to have $\kappa\ell \to \infty$ and $\kappa\eta \to 0$ simultaneously, so that we expect that (8.3.1) and (8.3.5) can be matched. Equating the two and using $\kappa\ell = R_\ell^n$, $\kappa\eta \sim R_\ell^{n-3/4}$, we obtain

$$u^2 \ell F(R_\ell^n) = \nu^2 \eta f(R_\ell^{n-3/4}), \tag{8.3.9}$$

which becomes

$$R_\ell^{5/4} F(R_\ell^n) = f(R_\ell^{n-3/4}). \tag{8.3.10}$$

This has to be satisfied for any n in the interval between 0 and 3/4. The solution of (8.3.10) is

$$F(\kappa\ell) = \alpha(\kappa\ell)^{-5/3}, \quad f(\kappa\eta) = \alpha(\kappa\eta)^{-5/3}. \tag{8.3.11}$$

In the literature, this spectrum is often presented in nonnormalized form. Substitution of (8.3.11) into (8.3.1) or (8.3.5) gives

$$E(\kappa) = \alpha\epsilon^{2/3}\kappa^{-5/3}. \tag{8.3.12}$$

This expression is valid for $\kappa\ell \to \infty$, $\kappa\eta \to 0$, $R_\ell \to \infty$. Experimental data indicate that $\alpha = 1.5$ approximately. The range of wave numbers for which (8.3.12) is valid is called the *inertial subrange*; it is the spectral equivalent of the inertial sublayer in boundary layers. In the inertial subrange, the one-dimensional spectra F_{11} and F_{22} are also proportional to $\epsilon^{2/3}\kappa_1^{-5/3}$.

With (8.3.11), the conditions (8.3.6, 8.3.7) become

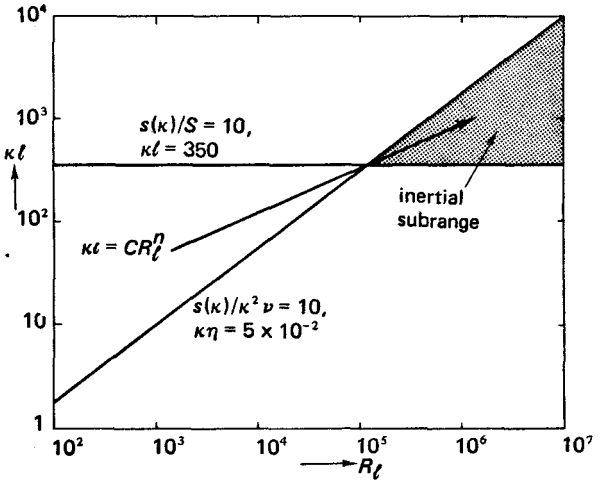

Figure 8.6. The inertial subrange.

$$\frac{s(\kappa)}{S} = \frac{n^{1/2}}{2\pi} R_\ell^{2n/3} \to \infty, \tag{8.3.13}$$

$$\frac{s(\kappa)}{2} = \frac{n^{1/2}}{2\pi} R_\ell^{1-4n/3} \to \infty, \tag{8.3.14}$$

so that these are indeed satisfied if $R_\ell \to \infty$ and $0 < n < 3/4$.

Recall that the mean velocity profile in the inertial sublayer can be obtained simply by postulating that $\partial U/\partial y$ is a function of u_* and y only. As we found in Section 5.2, this gives $\partial U/\partial y = u_*/\kappa y$. In a similar way, (8.3.12) can be obtained simply by postulating that $E = E(\epsilon,\kappa)$ for $1/\ell \ll \kappa \ll 1/\eta$. The point of obtaining (8.3.12) with such care is to delineate the conditions of its validity. A graphical representation of these conditions is given in Figure 8.6. The horizontal line corresponds to $s(\kappa)/S = 10$, which makes the eddies of that size marginally independent of the mean strain rate S and therefore of the turbulence-production process ($\mathcal{P} = -\overline{u_i u_j} S_{ij}$). The line with a slope of $\frac{3}{4}$ corresponds to $s(\kappa)/\kappa^2\nu = 10$, which should make eddies of that size approximately independent of viscosity. It is clear that no inertial subrange exists unless the Reynolds number is quite large. With the conditions used previously, the Reynolds number needs to be at least 10^5; if the conditions are relaxed to $s(\kappa)/S > 3$, $s(\kappa)/\kappa^2\nu > 3$, the Reynolds number needs to be larger than 4×10^3. This is still a rather stringent condition. We conclude that it is unlikely that we would encounter an inertial subrange in laboratory flows;

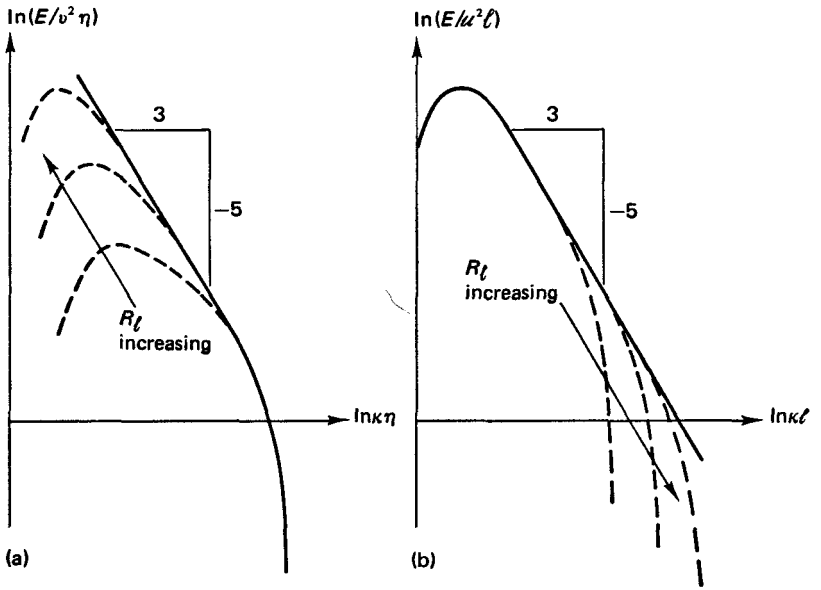

Figure 8.7. The spectrum of turbulence at different Reynolds numbers: (a) small-scale normalization, (b) large-scale normalization.

however, it is frequently observed in geophysical flows. The emergence of an inertial subrange in the spectrum of turbulence with increasing Reynolds numbers is sketched in Figure 8.7.

8.4
The effects of production and dissipation

In the inertial subrange, no energy is added by the mean flow and no energy is taken out by viscous dissipation, so that the energy flux T across each wave number is constant. In other words, the central part of the energy cascade is conservative, much like a cascade of waterfalls without any springs or drains. Because the total amount of energy dissipated per unit mass and time is ϵ, the spectral energy flux T in the inertial subrange is equal to ϵ.

In this section, we want to get a qualitative impression of how $E(\kappa)$ behaves near the ends of the inertial subrange. Recall that eddies of wave number κ get their energy, $\kappa E(\kappa)$, mainly from eddies of wave number 0.38κ, whose strain rate is $s(0.38\kappa) \cong \frac{1}{2}s(\kappa)$. The anisotropy produced by the larger

eddies is proportional to $s(0.38\kappa)/s(\kappa)$, so that the energy flux T may be represented by

$$T(\kappa) = \frac{8\pi}{\alpha^{3/2}} \kappa E(\kappa) \frac{s^2(0.38\kappa)}{s(\kappa)} = \frac{2\pi}{\alpha^{3/2}} \kappa E(\kappa) s(\kappa). \tag{8.4.1}$$

The numerical factor has been chosen in such a way that $T = \epsilon$ in the inertial subrange, with $s(\kappa) = (\kappa^3 E)^{1/2}/2\pi$ (8.2.6) and $E(\kappa) = \alpha\epsilon^{2/3}\kappa^{-5/3}$ (8.3.12).

Substituting (8.2.6) into (8.4.1), we may write T as

$$T(\kappa) = \alpha^{-3/2} E^{3/2} \kappa^{5/2}. \tag{8.4.2}$$

This gives some indication of the variation of T across the spectrum. If $E \propto \kappa^{n-5/3}$, then $T \propto \kappa^{3n/2}$, so that T increases when the spectrum decreases less rapidly than $\kappa^{-5/3}$ and decreases when E decreases more rapidly than $\kappa^{-5/3}$.

In the inertial subrange, $s(\kappa)$ is given by

$$s(\kappa) = \frac{(\kappa^3 E)^{1/2}}{2\pi} = \frac{\alpha^{1/2}}{2\pi} \epsilon^{1/3} \kappa^{2/3}. \tag{8.4.3}$$

It turns out to be convenient to use the right-hand side of (8.4.3) not only inside the inertial subrange but also beyond its edges. Substituting the right-hand side of (8.4.3) into (8.4.1), we obtain

$$T(\kappa) = \alpha^{-1} \epsilon^{1/3} \kappa^{5/3} E(\kappa). \tag{8.4.4}$$

This estimate of $T(\kappa)$, however crude it may be, is attractive because it represents the spectral flux at some wave number as a local flux, determined only by the value of E and the inertial time scale $\epsilon^{-1/3}\kappa^{-2/3}$ at that wave number, and because it makes the relation between T and E a linear one. Of course, (8.4.2) is also a local estimate for $T(\kappa)$; however, it is not linear in E, so that it produces poorly behaved spectra.

Before we use (8.4.4) to calculate spectra outside the inertial subrange, let us take a close look at the assumptions underlying (8.4.2) and (8.4.4). In the inertial subrange, $T = \epsilon = \alpha^{-1} E^{3/2} \kappa^{5/2}$; comparing this with (8.4.2), we see that we are relaxing the condition $T = \epsilon$. Clearly, (8.4.2) assumes that T is proportional to $E^{3/2}\kappa^{5/2}$ even if $T \neq \epsilon$. In other words, we use inertial scaling for T even though we are outside the inertial subrange. This approximation can be justified only if the effects of viscosity and those of the mean strain rate are small, so that the difference between T and ϵ is small. Equation

(8.4.4) is even cruder, because it relaxes the condition $T = \epsilon$ but retains the inertial-subrange expression for the strain rate.

Both (8.4.2) and (8.4.4) may be thought of as spectral interpretations of mixing-length theory. If $-\overline{uv} \sim u\ell\, \partial U/\partial y$, the production of turbulent energy is proportional to $u\ell(\partial U/\partial y)^2$. Making the substitutions $u \to (\kappa E)^{1/2}$, $\ell \to 1/\kappa$, and $(\partial U/\partial y)^2 \to \kappa^2(\kappa E)$, we obtain (8.4.2); of course, turbulence production is now interpreted as transfer of energy from larger eddies to smaller eddies rather than transfer from the mean flow to all eddies. In a similar way, if we use $\epsilon \sim u^3/\ell$ to substitute for u in $u\ell(\partial U/\partial y)^2$, we obtain $\epsilon^{1/3}\ell^{4/3}(\partial U/\partial y)^2$. With $\ell \to 1/\kappa$ and $(\partial U/\partial y)^2 \to \kappa^2(\kappa E)$, this produces (8.4.4). Realizing how crude mixing-length theory is, we should not be too concerned about the relative merits of (8.4.2) and (8.4.4). It should be kept in mind that these spectral mixing-length models, like their spatial counterparts, can be used only in situations with a single length scale and a single time scale.

The effect of dissipation The viscous dissipation in a wave-number interval $d\kappa$ is equal to $2\nu\kappa^2 E(\kappa)\, d\kappa$, as we found in (8.3.2). This loss of energy is taken out of the energy flux $T(\kappa)$, so that we must have

$$dT/d\kappa = -2\nu\kappa^2 E. \tag{8.4.5}$$

If we substitute for $T(\kappa)$ with (8.4.4) and integrate the resulting equation, we obtain

$$E(\kappa) = \alpha\epsilon^{2/3}\kappa^{-5/3} \exp[-\tfrac{3}{2}\alpha(\kappa\eta)^{4/3}]. \tag{8.4.6}$$

This result, first given by Corrsin (1964) and later by Pao (1965), agrees very well with experimental data up to the largest values of $\kappa\eta$ that have been measured. Because virtually no data are available beyond $\kappa\eta = 1$, this is not a very severe test. In fact, the use of $s(\kappa) \sim \epsilon^{1/3}\kappa^{2/3}$ is unwarranted beyond $\kappa\eta = 1$ because viscosity limits the maximum strain rate to $(\epsilon/\nu)^{1/2}$. Also, of course, the use of (8.4.2) in a region in which viscous time scales are important is incorrect. The exponential decay of (8.4.6), which allows it to be integrated or differentiated without creating problems at large $\kappa\eta$, is thus merely a happy coincidence.

The dissipation spectrum corresponding to (8.4.6) is

$$D(\kappa) = 2\nu\kappa^2 E(\kappa) = 2\alpha\, \nu\epsilon^{2/3}\kappa^{1/3} \exp[-\tfrac{3}{2}\alpha(\kappa\eta)^{4/3}]. \tag{8.4.7}$$

In the inertial subrange ($\kappa\eta \ll 1$), the dissipation spectrum is proportional to

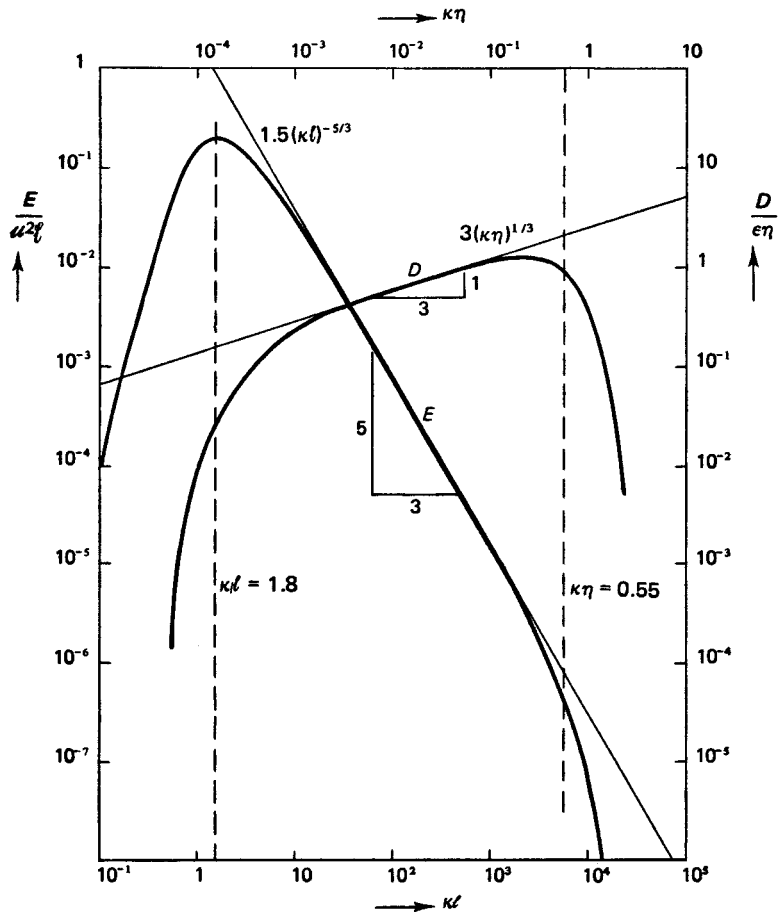

Figure 8.8. Normalized energy and dissipation spectra for $R_\ell = 2 \times 10^5$. The dashed lines indicate cutoffs for the approximate spectra to be described later.

$\kappa^{1/3}$. Figure 8.8 gives an impression of the shapes of $E(\kappa)$ and $D(\kappa)$. The curves also show how $E(\kappa)$ and $D(\kappa)$ trail off at low wave numbers; the analysis leading to this follows.

If $\alpha = 1.5$, the peak of the dissipation spectrum occurs at $\kappa\eta = 0.2$ and the value of $D(\kappa)$ at the peak is $D = 1.4\epsilon\eta$. These numbers agree well with most of the experimental data.

The effect of production Eddies near the lower edge of the inertial subrange, where $\kappa\ell$ is not necessarily very large, receive most of their energy from slightly larger eddies, but they also absorb some energy directly from the strain rate S of the mean flow. The anisotropy induced by the mean strain rate in eddies of wave number κ is proportional to $S/s(\kappa)$, so that the work done by the mean strain rate per unit wave number and per unit time is proportional to $ES^2/s(\kappa)$. Using (8.4.3) to substitute for $s(\kappa)$, we obtain for the production spectrum $P(\kappa)$,

$$P(\kappa) = \frac{2\pi\beta}{\alpha^{1/2}} \frac{S^2}{\epsilon^{1/3}} \kappa^{-2/3} E(\kappa). \tag{8.4.8}$$

The constant β is undetermined. In the inertial subrange, the production spectrum is proportional to $\kappa^{-7/3}$; this agrees fairly well with experimental evidence.

The spectral energy transfer $T(\kappa)$ increases wherever energy is being added. If the total amount of energy does not change and if viscous dissipation can be neglected, we have

$$dT/d\kappa = P(\kappa). \tag{8.4.9}$$

When (8.4.4) and (8.4.8) are substituted into (8.4.9), there results, after the equation is integrated,

$$E(\kappa) = \alpha\epsilon^{2/3}\kappa^{-5/3} \exp[-\tfrac{3}{2}\pi\beta\alpha^{1/2}(\kappa\ell)^{-4/3}]. \tag{8.4.10}$$

Here we have defined ℓ by $\ell = u^3/\epsilon$ and we have taken $S = u/\ell$ for convenience, as in (8.3.5). Although (8.4.10) is well behaved at all wave numbers, the assumptions $s(\kappa) \sim \epsilon^{1/3}\kappa^{2/3}$ and (8.4.8) on which it is based are not valid for small values of $\kappa\ell$. The value of β can be determined by requiring that the integral of (8.4.10) be equal to the total energy $\frac{1}{2}\overline{u_i u_i} = \frac{3}{2}u^2$; this yields $\beta = 0.3$. The maximum of (8.4.10) occurs at $\kappa\ell = 1.3$ approximately; its value

is about $0.2u^2\ell$. Figure 8.8 gives a sketch of $E(\kappa)$ and $D(\kappa) = 2\nu\kappa^2 E(\kappa)$ as predicted by (8.4.10). These curves are in qualitative agreement with most experimental data. The Reynolds number in Figure 8.8 is $R_\ell = 2 \times 10^5$, which corresponds to $\ell/\eta = 10^4$. The graph suggests that there are only about two decades of inertial subrange at this Reynolds number.

Approximate spectra for large Reynolds numbers From the appearance of Figure 8.8 we are tempted to approximate $E(\kappa)$ by $1.5u^2\ell(\kappa\ell)^{-5/3}$ between a wave number somewhere near $\kappa\ell = 1$ and a wave number near $\kappa\eta = 1$, and to put it equal to zero outside that range. In fact, for many purposes such an approximation is quite satisfactory, provided that the Reynolds number is large enough.

Of course, the spectrum should have a correct integral. If the limits of integration of the truncated spectrum are κ_0 and κ_d, we have

$$\frac{3}{2}u^2 = \int_0^\infty E(\kappa)\,d\kappa \cong \int_{\kappa_0}^{\kappa_d} 1.5u^2\ell(\kappa\ell)^{-5/3}\,d\kappa \cong 1.5u^2\int_{\kappa_0\ell}^{\infty} x^{-5/3}\,dx. \qquad (8.4.11)$$

We may set the upper limit of integration equal to ∞ if ℓ/η is large. This requires large Reynolds numbers. The integral condition (8.4.11) serves to determine $\kappa_0\ell$; the result is $\kappa_0\ell = (\frac{3}{2})^{3/2} \cong 1.8$. The other end of the range can be determined by requiring that the integral of the dissipation spectrum be correct. We can write

$$\epsilon = \int_0^\infty D(\kappa)\,d\kappa \cong \int_{\kappa_0}^{\kappa_d} 3\epsilon\eta(\kappa\eta)^{1/3}\,d\kappa \cong 3\epsilon\int_0^{\kappa_d\eta} x^{1/3}\,dx. \qquad (8.4.12)$$

The lower limit has been put at zero because the Reynolds number is presumed to be large. From (8.4.12), we obtain $\kappa_d\eta = 0.55$ approximately. The cutoffs $\kappa_0\ell = 1.8$ and $\kappa_d\eta = 0.55$ are indicated with dashed vertical lines in Figure 8.8.

The one-dimensional spectra (F_{11} and F_{22}) corresponding to this truncated three-dimensional spectrum can be computed fairly easily if we assume that the turbulence is isotropic. Because $E(\kappa)$ is equal to zero in the range $0 \leqslant \kappa\ell < 1.8$, F_{11} curves parabolically downward in that range (8.1.18) and F_{22} curves parabolically upward (8.1.19). In the range where $E(\kappa) \propto \kappa^{-5/3}$, F_{11} and F_{22} have the same slope (see Section 8.1); the coefficients involved can be computed with the isotropic relations (8.1.13, 8.1.14). For $0 \leqslant \kappa_1\ell < \kappa_0\ell$, there results

$$F_{11}(\kappa_1) = \tfrac{33}{110}\,\alpha u^2 \ell (\kappa_0 \ell)^{-5/3}\,[1 - \tfrac{5}{11}\,(\kappa_1/\kappa_0)^2], \tag{8.4.13}$$

$$F_{22}(\kappa_1) = \tfrac{1}{2} \cdot \tfrac{33}{110}\,\alpha u^2 \ell (\kappa_0 \ell)^{-5/3}\,[1 + \tfrac{5}{11}\,(\kappa_1/\kappa_0)^2]. \tag{8.4.14}$$

For $\kappa_1 \ell > \kappa_0 \ell$, the results are

$$F_{11}(\kappa_1) = \tfrac{9}{55}\,\alpha u^2 \ell (\kappa_1 \ell)^{-5/3} \tag{8.4.15}$$

$$F_{22}(\kappa_1) = \tfrac{4}{3}\,F_{11}(\kappa_1) = \tfrac{4}{3} \cdot \tfrac{9}{55}\,\alpha u^2 \ell (\kappa_1 \ell)^{-5/3}. \tag{8.4.16}$$

Of course, F_{11} and F_{22} are truncated at the same point as E; that is, $\kappa_1 \eta = 0.55$. The integrals of F_{11} and F_{22} over all κ_1 are equal to u^2 by virtue of (8.1.6, 8.1.7), so that the integrals of F_{11} and F_{22} over all positive κ_1 are equal to $\frac{1}{2}u^2$. In the literature, F_{11} and F_{22} are sometimes normalized in such a way that their integrals over all positive κ_1 are equal to u^2; in that case, the coefficient $\frac{9}{55}$ in (8.4.15, 8.4.16) becomes $\frac{18}{55}$, with corresponding changes in (8.4.13) and (8.4.14). Note that (8.4.13–8.4.16) describe F_{11} and F_{22} for $\kappa_1 > 0$. The spectra given by (8.4.13–8.4.16) are sketched in Figure 8.9. The parabolic part of F_{11} matches the $\kappa^{-5/3}$ part at κ_0 without a discontinuity of slope, but the slope of F_{22} changes sign at κ_0.

The values of F_{11} and F_{22} at the origin ($\kappa_1 = 0$) are of interest because they determine the longitudinal and transverse integral scales L_{11} and L_{22}:

$$F_{11}(0) = \frac{1}{2\pi} \int_{-\infty}^{\infty} R_{11}(r, 0, 0)\, dr = \frac{u^2}{\pi} L_{11}, \tag{8.4.17}$$

$$F_{22}(0) = \frac{1}{2\pi} \int_{-\infty}^{\infty} R_{22}(r, 0, 0)\, dr = \frac{u^2}{\pi} L_{22}. \tag{8.4.18}$$

Note that integral scales are defined as the integral of the correlation between zero and positive infinity, so that the factor $1/2\pi$ in front of the integrals becomes $1/\pi$ at the right-hand side of (8.4.17, 8.4.18). Evaluating $F_{11}(0)$ and $F_{22}(0)$ from (8.4.13, 8.4.14) and using $\alpha = 1.5$ and $\kappa_0 \ell = (\frac{3}{2})^{3/2}$, we obtain

$$L_{11} = \ell/2, \quad L_{22} = \ell/4. \tag{8.4.19}$$

We recall that ℓ was defined by $\epsilon = u^3/\ell$. The relations between these length scales and the Lagrangian integral time scale are derived in the next section. Although (8.4.19) was derived for isotropic turbulence, it may be used also to obtain crude estimates in shear flows.

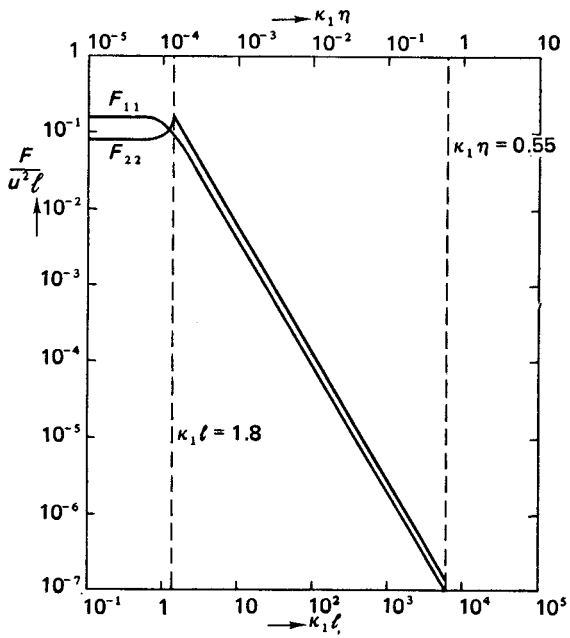

Figure 8.9. Crude approximations for the one-dimensional spectra at $R_\ell = 2 \times 10^5$ ($\ell/\eta = 10^4$).

8.5
Time spectra

So far we have discussed only space spectra, which are Fourier transforms of autocorrelations taken with a spatial separation and zero time delay. We now want to consider time spectra, which are obtained from correlations taken at the same point with varying time delay. If the point of measurement is a fixed point in a coordinate system chosen such that the mean velocity is zero, we obtain an *Eulerian time spectrum*; if the point of measurement is a wandering material point, we obtain a *Lagrangian time spectrum*. The measurements needed to obtain these spectra are quite difficult and time-consuming; very few experimental data are available.

Because time is a one-dimensional variable, time spectra are one-dimensional. We can have time spectra of u_1, u_2, or u_3; however, we are mainly interested in spectra which integrate to the total energy $\frac{1}{2}\overline{u_i u_i} = \frac{3}{2}u^2$. Let us define the Eulerian time spectrum $\psi_{ij}(\omega)$ by

$$\overline{u_i(\mathbf{x}, t)u_j(\mathbf{x}, t+\tau)} = R_{ij}(\tau) = \int_{-\infty}^{\infty} \exp(i\omega\tau)\, \psi_{ij}(\omega)\, d\omega,$$

$$\psi_{ij}(\omega) = \frac{1}{2\pi} \int_{-\infty}^{\infty} \exp(-i\omega\tau)\, R_{ij}(\tau)\, d\tau. \tag{8.5.1}$$

The Lagrangian time spectrum $\chi_{ij}(\omega)$ can be defined by

$$\overline{v_i(\mathbf{a}, t)v_j(\mathbf{a}, t+\tau)} = \mathscr{R}_{ij}(\tau) = \int_{-\infty}^{\infty} \exp(i\omega\tau)\, \chi_{ij}(\omega)\, d\omega,$$

$$\chi_{ij}(\omega) = \frac{1}{2\pi} \int_{-\infty}^{\infty} \exp(-i\omega\tau)\, \mathscr{R}_{ij}(\tau)\, d\tau. \tag{8.5.2}$$

In homogeneous turbulence, $\overline{u_i u_i} = \overline{v_i v_i}$ (see Section 7.2), so that

$$\int_{-\infty}^{\infty} \psi_{ii}(\omega)\, d\omega = \int_{-\infty}^{\infty} \chi_{ii}(\omega)\, d\omega = \overline{u_i u_i} = 3u^2. \tag{8.5.3}$$

If the turbulence is also isotropic, $\psi_{11} = \psi_{22} = \psi_{33}$ and $\chi_{11} = \chi_{22} = \chi_{33}$. These spectra do not vanish at the origin; instead, their values at $\omega = 0$ define integral time scales:

$$\psi_{ii}(0) = \frac{1}{2\pi} \int_{-\infty}^{\infty} R_{ii}(\tau)\, d\tau = \frac{\overline{u_i u_i}}{\pi}\, T = \frac{3u^2}{\pi}\, T, \tag{8.5.4}$$

$$\chi_{ii}(0) = \frac{1}{2\pi} \int_{-\infty}^{\infty} \mathscr{R}_{ii}(\tau)\, d\tau = \frac{\overline{u_i u_i}}{\pi}\, \mathscr{T} = \frac{3u^2}{\pi}\, \mathscr{T}. \tag{8.5.5}$$

Here, T is the Eulerian integral time scale and $\mathscr{T}$ is the Lagrangian integral time scale. It would be necessary to define more than one T and more than one $\mathscr{T}$ if the turbulence were not homogeneous and isotropic.

In order to understand what these time spectra mean, we have to use the energy cascade concept. We found in Section 8.2 that each eddy size or wave number is associated with a particular time scale and that the time scale decreases with increasing wave number over most of the spectrum. If each eddy can be assigned a size and a time scale, either one can be used to identify its position in the time spectrum and in the space spectrum. Therefore, the time spectrum should be a simple rearrangement of the space spectrum in terms of time scales.

One problem arises. In the dissipative end of the space spectrum, the time scale $1/s(\kappa) \sim (\kappa^3 E)^{-1/2}$ (8.2.6) increases with increasing wave number. This

means that the relation between size and time scale is not monotone near $\kappa\eta = 1$: the time scale decreases first, but increases beyond the peak of the dissipation spectrum. Therefore, if the energy in the space spectrum is rearranged by time scale or frequency, there are two contributions at a given frequency. One contribution comes from a relatively low wave number, where eddies are inviscid, the other comes from a wave number in the dissipative range, where eddies are dominated by viscosity. However, the energy in the dissipation range is very small compared to that at smaller wave numbers; it can safely be ignored. Even at very large time scales, which receive contributions from $\kappa\ell \ll 1$ and $\kappa\eta \gg 1$, the energy of the large eddies is large compared to that of the very small eddies because the spectrum in the dissipation range decreases much more rapidly than that below $\kappa\ell = 1$.

We conclude that we may treat the time spectrum as a rearrangement of the space spectrum wherever viscous effects can be ignored. Because time scales are monotone decreasing with wave number (except in the dissipation range), we expect that the mean flow does not affect the spectrum at frequencies much larger than the mean strain rate S. Hence, the two time spectra have an equilibrium range at high frequencies if the Reynolds number is large enough. Of course, the turbulence should be isotropic in that range. The spectra in the equilibrium range have to be normalized with ϵ and ν; there results

$$\psi_{ii}(\omega) = v\eta\, f(\omega\eta/v), \quad \chi_{ii}(\omega) = v\eta\, f'(\omega\eta/v). \tag{8.5.6}$$

Here, $v = (\nu\epsilon)^{1/4}$ and $\eta = (\nu^3/\epsilon)^{1/4}$ are the familiar Kolmogorov velocity and length. The nondimensional frequency $\omega\eta/v$ is equal to $\omega(\nu/\epsilon)^{1/2} \sim \omega\lambda/u$ (λ is the Taylor microscale); it seems only proper to nondimensionalize frequencies with the smallest time scale of turbulence.

The idea that equilibrium-range scaling can be applied to time spectra was first suggested by Inoue (1951). Because no time spectra of this kind have ever been measured, it is not known how well justified the reasoning is. The dissipative mechanism is quite different in Eulerian and Lagrangian variables, so that we do not expect the forms of f and f' to be the same in the dissipation range.

In the energy-containing range, the time spectra should scale with u and ℓ if the contributions of eddies from the dissipation range in the space spectrum can be neglected. Therefore, we should be permitted to write, for $\omega(\nu/\epsilon)^{1/2} \ll 1$,

$$\psi_{ii}(\omega) = u\ell F(\omega\ell/u), \quad \chi_{ii}(\omega) = u\ell\mathcal{F}(\omega\ell/u). \tag{8.5.7}$$

Again the shapes of F and $\mathcal{F}$ are probably different because the lowest frequencies seen by a fixed point and by a wandering point are determined by different mechanisms.

The inertial subrange If the Reynolds number is so large that the high-frequency end of (8.5.7) overlaps with the low-frequency end of (8.5.6), there should be an inertial subrange in ψ_{ii} and in χ_{ii}. In the inertial subrange, ψ_{ii} and χ_{ii} should be independent of the viscous frequency (strain rate) $v/\eta = (\epsilon/\nu)^{1/2}$ and of the large-eddy frequency u/ℓ. If this is the case, $\psi_{ii} = \psi_{ii}(\epsilon,\omega)$ and $\chi_{ii} = \chi_{ii}(\epsilon,\omega)$, so that the inertial subrange in the time spectra must be given by

$$\psi_{ii} = B\epsilon\omega^{-2}, \quad \chi_{ii} = \beta\epsilon\omega^{-2}. \tag{8.5.8}$$

The constants B and β are unknown; they can be estimated only if we accept the premise that the time spectra are simple rearrangements of $E(\kappa)$. With this premise, we should put $B = \beta$. Also, if the energy at wave number κ is $\kappa E(\kappa)$ and if the angular frequency corresponding to κ is $2\pi s(\kappa) = \alpha^{1/2}\epsilon^{1/3}\kappa^{2/3}$ (8.4.3), we should have

$$\kappa E = \omega\psi_{ii} = \omega\chi_{ii}, \tag{8.5.9}$$

$$2\pi s(\kappa) = \alpha^{1/2}\epsilon^{1/3}\kappa^{2/3} = \omega. \tag{8.5.10}$$

Eliminating κ between (8.5.9) and (8.5.10) and using $E(\kappa) = \alpha\epsilon^{2/3}\kappa^{-5/3}$, we obtain

$$\psi_{ii} = \chi_{ii} = \alpha^{3/2}\epsilon\omega^{-2}. \tag{8.5.11}$$

With $\alpha = 1.5$, we find $B = \beta = 1.8$.

The Lagrangian integral time scale The form of the time spectra at low frequencies (below the inertial subrange) is more difficult to predict. We are mainly interested in the Lagrangian spectrum, because we could use it to predict the Lagrangian integral scale. However, if we understood Lagrangian dynamics well enough to derive a spectrum, we would probably not need to estimate the Lagrangian integral scale in this way. Lacking any information other than that $\chi_{ii}(0)$ should be finite, the best we can do is to guess that χ_{ii}

is constant for all frequencies below some ω_0 and that it follows (8.5.11) above ω_0. Thus, let us assume that

$$\chi_{ii} = \beta\epsilon\omega_0^{-2} \text{ for } 0 \leqslant \omega < \omega_0, \tag{8.5.12}$$

$$\chi_{ii} = \beta\epsilon\omega^{-2} \text{ for } \omega \geqslant \omega_0. \tag{8.5.13}$$

The value of ω_0 can be determined by requiring that the integral of $\chi_{ii}(\omega)$ over all ω be equal to $\overline{u_i u_i} = 3u^2$ (8.5.3). If the Reynolds number is so large that the viscous cutoff can be ignored, there results

$$\omega_0 \ell/u = 4\beta/3 \cong 2.4. \tag{8.5.14}$$

The resulting value of $\mathcal{T}$ is approximately $\ell/3u$. Using the Eulerian length scales L_{11} and L_{22} obtained in (8.4.19), we find

$$\mathcal{T} \cong \frac{1}{3}\frac{\ell}{u} \cong \frac{2}{3}\frac{L_{11}}{u} \cong \frac{4}{3}\frac{L_{22}}{u}. \tag{8.5.15}$$

This method of estimating the Lagrangian integral scale was first suggested by S. Corrsin (1963a); his result was somewhat different because he used $\chi_{ii} = 0$ for $0 < \omega < \omega_0$. Considering the crudeness of the assumptions involved in obtaining (8.5.15), we should not take the values of the coefficients too seriously. In effect, (8.5.15) gives barely more than the dimensional statement $\mathcal{T} \sim L_{11}/u \sim L_{22}/u$. It may be taken as a warning that this analysis cannot distinguish between $\mathcal{T}$ and T. Intuition suggests that $\mathcal{T} > T$: a wandering point should tend to maintain its original velocity somewhat longer than the velocity at a fixed point in space. In any case, in the absence of better estimates, (8.5.15) is useful for the purpose of obtaining Lagrangian integral scales from Eulerian correlation data; recall that a value for $\mathcal{T}$ is needed in the prediction of turbulent transport (Section 7.1).

An approximate Lagrangian spectrum Equations (8.5.12–8.5.14) define a crude approximation to the Lagrangian time spectrum, in the spirit of the one-dimensional spectra presented in Figure 8.9. One detail yet needs to be resolved: the spectrum has to be truncated at some frequency in the dissipation range. Because the Lagrangian dynamics of dissipation cannot be formulated in simple terms, we can do no more than compute the maximum value of $\omega = 2\pi s(\kappa) = (\kappa^3 E)^{1/2}$ from Corrsin's form (8.4.6) of the Eulerian space spectrum. If $\alpha = 1.5$, this maximum occurs at $\kappa\eta = 1$; its value is

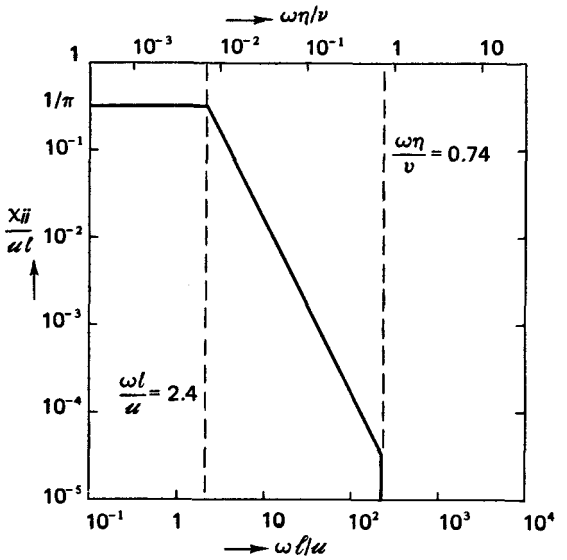

Figure 8.10. An approximate Lagrangian spectrum for $R_\ell = 10^5$.

$$\omega_d = 0.74(\epsilon/\nu)^{1/2} = 0.74\nu/\eta. \tag{8.5.16}$$

This is in agreement with the ideas developed in Chapter 3; that is, the maximum frequency (vorticity, strain rate) is of order $(\epsilon/\nu)^{1/2}$. The ratio between ω_d and ω_0 is, from (8.5.14) and (8.5.16),

$$\omega_d/\omega_0 = 0.31\ (\epsilon/\nu)^{1/2}\ \ell/u = 0.31\ R_\ell^{1/2}. \tag{8.5.17}$$

The approximate Lagrangian spectrum for $R_\ell = 10^5$, $\omega_d/\omega_0 \sim 10^2$ is sketched in Figure 8.10. The separation of scales in the time spectrum is much less than that in the space spectrum; indeed, ω_d/ω_0 is a much better measure of the extent of the inertial subrange because vorticities and strain rates, which are frequencies, dominate the dynamics of turbulence.

8.6
Spectra of passive scalar contaminants

When a dynamically passive contaminant is mixed by a turbulent flow, a spectrum of contaminant fluctuations is produced. The scales of contaminant fluctuations range from the scale of the energy-containing eddies to a smallest

scale that depends on the ratio of diffusivities (Prandtl number, Schmidt number), as we found in Sections 3.4 and 7.3. Many of the concepts that were used to elucidate the form of the kinetic energy spectrum can also be applied to the spectra of scalar contaminants; we shall find that these spectra have simple forms in various wave-number ranges if the Reynolds number is large. To simplify the discussion, we assume that the passive contaminant is heat. If the temperature fluctuations are small enough, the associated buoyancy is dynamically unimportant.

One- and three-dimensional spectra Passive scalar contaminants have one- and three-dimensional spectra. These spectra are defined in a similar way as velocity spectra, but they are simpler because there is only one variable, rather than three components, to be accounted for. If $\theta(\mathbf{x},t)$ is a temperature fluctuation, the spatial autocorrelation $R_\theta(\mathbf{r})$ is defined by

$$R_\theta(\mathbf{r}) = \overline{\theta(\mathbf{x}, t)\theta(\mathbf{x}+\mathbf{r}, t)}. \tag{8.6.1}$$

The Fourier transform of $R_\theta(\mathbf{r})$ is the spatial spectrum $\phi(\boldsymbol{\kappa})$:

$$R_\theta(\mathbf{r}) = \iiint_{-\infty}^{\infty} \exp(i\boldsymbol{\kappa}\cdot\mathbf{r})\,\phi_\theta(\boldsymbol{\kappa})\,d\boldsymbol{\kappa},$$

$$\phi_\theta(\boldsymbol{\kappa}) = \frac{1}{(2\pi)^3}\iiint_{-\infty}^{\infty} \exp(-i\boldsymbol{\kappa}\cdot\mathbf{r})\,R_\theta(\mathbf{r})\,d\mathbf{r}. \tag{8.6.2}$$

Just as for the velocity field, $\phi_\theta(\boldsymbol{\kappa})$ is the "energy" of waves of wave-number vector $\boldsymbol{\kappa}$. A *one-dimensional* spectrum $F_\theta(\kappa_1)$ may be defined by

$$R_\theta(r, 0, 0) \equiv \int_{-\infty}^{\infty} \exp(i\kappa_1 r)\,F_\theta(\kappa_1)\,d\kappa_1. \tag{8.6.3}$$

The relation between $\phi_\theta(\boldsymbol{\kappa})$ and $F_\theta(\kappa_1)$ is given by

$$\begin{aligned} R_\theta(r, 0, 0) &= \iiint_{-\infty}^{\infty} \exp(i\kappa_1 r)\,\phi_\theta(\boldsymbol{\kappa})\,d\boldsymbol{\kappa} \\ &= \int_{-\infty}^{\infty} \exp(i\kappa_1 r)\left(\iint_{-\infty}^{\infty} \phi_\theta\,d\kappa_2\,d\kappa_3\right)d\kappa_1, \end{aligned} \tag{8.6.4}$$

$$F_\theta(\kappa_1) = \iint_{-\infty}^{\infty} \phi_\theta\,d\kappa_2\,d\kappa_3. \tag{8.6.5}$$

Clearly, $F_\theta(\kappa_1)$ suffers from the same aliasing problem as the one-dimensional spectra for the velocity (see (8.1.9)).

The *three-dimensional* spectrum $E_\theta(\kappa)$ is defined as the spectral density of waves which have the same wave-number magnitude κ ($\kappa^2 = \boldsymbol{\kappa}\cdot\boldsymbol{\kappa} = \kappa_j\kappa_j$), regardless of direction. This is obtained by integrating $\phi_\theta(\boldsymbol{\kappa})$ over a sphere with radius κ (see 8.1.4):

$$E_\theta(\kappa) = \oiint \tfrac{1}{2}\phi_\theta \, d\sigma, \tag{8.6.6}$$

$$\tfrac{1}{2}\overline{\theta^2} = \int_0^\infty E_\theta(\kappa)\, d\kappa. \tag{8.6.7}$$

Because the integral of E_θ is $\frac{1}{2}\overline{\theta^2}$, we call E_θ the spectrum of temperature variance.

In an isotropic field, there is only one one-dimensional spectrum because the direction of the spatial separation $\mathbf{r}$ in $R_\theta(\mathbf{r})$ is immaterial. For the same reason, $\phi_\theta(\boldsymbol{\kappa})$ depends only on the wave-number modulus κ under isotropic conditions. The isotropic relations between $F_\theta(\kappa_1)$, $\phi_\theta(\kappa)$, and $E_\theta(\kappa)$ are (Hinze, 1959)

$$E_\theta(\kappa) = 2\pi\kappa^2\phi_\theta(\kappa), \tag{8.6.8}$$

$$F_\theta(\kappa_1) = \int_{\kappa_1}^\infty \kappa^{-1}E_\theta(\kappa)\, d\kappa, \quad E_\theta(\kappa) = -\kappa\frac{d}{d\kappa}[F_\theta(\kappa)]. \tag{8.6.9}$$

If the temperature field has a finite integral scale, $F_\theta(0)$ is finite and $E_\theta(\kappa)$ begins parabolically upward from $\kappa = 0$ (recall that the kinetic energy spectrum starts quartically from $\kappa = 0$). This statement is valid even if the field is not isotropic.

The cascade in the temperature spectrum In the development of a model for the spectral transfer of temperature fluctuations, we use E and E_θ, because they represent the "energy" at a given wave number without effects due to aliasing. If the Reynolds number is large enough for an equilibrium range to exist in the kinetic energy spectrum, there is also an equilibrium range, exhibiting local isotropy, in the spectrum of temperature variance, because it is the turbulent motion that is mixing the temperature field.

The cascade in the temperature spectrum is similar to that in the velocity spectrum. The temperature gradient associated with an eddy of wave number

κ_1 is of order $[\kappa_1^3 E_\theta(\kappa_1)]^{1/2}$. The velocity fluctuations of the eddies of the next smaller scale ($\kappa_2 > \kappa_1$, say), distort this gradient, thus producing temperature fluctuations of smaller scale. This is like the production of temperature variance from a mean temperature gradient, which we discussed in Section 3.4. There, temperature variance was produced at a rate $-\overline{\theta u_j}\,\partial\Theta/\partial x_j$; perhaps we can reason by analogy here. The spatial heat flux θu_j was estimated as $u\ell\partial\Theta/\partial x_j$ in Chapter 2; the spectral flux of temperature variance thus should be the spectral equivalent of $u\ell(\partial\Theta/\partial x_j)^2$. Now, u and ℓ have to be substituted by the velocity $[\kappa_2 E(\kappa_2)]^{1/2}$ and the size $1/\kappa_2$ of the smaller eddies that distort the temperature gradients of the larger eddies. The spectral flux of temperature variance may then be estimated as

$$T_\theta = C\kappa_2^{-1}[\kappa_2 E(\kappa_2)]^{1/2}\kappa_1^3 E_\theta(\kappa_1). \tag{8.6.10}$$

If we ignore the difference between κ_1 and κ_2 because they are fairly close together, we obtain

$$T_\theta(\kappa) = C\kappa^2 E_\theta(\kappa E)^{1/2}. \tag{8.6.11}$$

This local estimate of T_θ is, of course, as crude as the cascade model developed for the kinetic energy spectrum. In particular, the significance at large and small wave numbers of scales associated with such quantities as kinematic viscosity ν, the thermal diffusivity γ, and the mean strain rate S is ignored.

Spectra in the equilibrium range Within the equilibrium range, $E_\theta(\kappa)$ should scale with the parameters governing the velocity field, which are ϵ and ν, and the corresponding parameters for the temperature field. The dissipation of temperature variance will be called N; it is defined by

$$N \equiv \gamma\,\overline{\frac{\partial\theta}{\partial x_i}\frac{\partial\theta}{\partial x_i}}. \tag{8.6.12}$$

Thus, we expect $E_\theta = E_\theta(\kappa,\epsilon,\nu,\gamma,N)$ in the equilibrium range. A convenient combination of variables is

$$E_\theta(\kappa) = N\epsilon^{-1/3}\kappa^{-5/3} f(\kappa\eta, \sigma). \tag{8.6.13}$$

Here, $\sigma = \nu/\gamma$ is the Prandtl number. Because of the presence of σ, the nondimensional spectrum f is different in different fluids.

If the Reynolds number is so large that the energy spectrum has an inertial subrange and if γ is small enough, so that there is an appreciable part of the spectrum where the thermal diffusivity is unimportant, we obtain an *inertial-convective subrange,* that is, an inertial range in which temperature fluctuations are simply convected. In this range, the spectrum should be independent of ν and γ, so that we have $E_\theta = E_\theta(\kappa, N, \epsilon)$, which can have only one form:

$$E_\theta(\kappa) = \beta N \epsilon^{-1/3} \kappa^{-5/3}. \tag{8.6.14}$$

This was first suggested independently by Corrsin (1951) and by Oboukhov (1949). Recent measurements give $\beta = 0.5$ approximately. If we substitute (8.6.14) and $E(\kappa) = \alpha \epsilon^{2/3} \kappa^{-5/3}$ into the estimate for T_θ given in (8.6.11), we find that the spectral transfer of temperature variance in the inertial-convective subrange is constant, as it should be. Conversely, if we assume that $T_\theta(\kappa) = N$, we obtain (8.6.14) from (8.6.11). In other words, the "mixing-length" model for T_θ given by (8.6.11) is consistent with (8.6.14).

If we want to take the effects of γ and ν into account, we have to distinguish between fluids with small Prandtl numbers and those with large Prandtl numbers. If $\sigma < 1$, so that $\gamma < \nu$, the thermal diffusivity becomes important within the inertial subrange, where the viscosity does not yet influence the spectrum. As in Section 3.4, we denote the Kolmogorov microscale for the temperature field by η_θ; recall that $\eta_\theta > \eta$ if $\gamma > \nu$ and that $\eta_\theta < \eta$ if $\gamma < \nu$. If $\gamma \gg \nu$, there is a range of wave numbers where $\kappa\eta_\theta \geqslant 1$, but $\kappa\eta \ll 1$. This is called an *inertial-diffusive subrange*; it occurs in mercury, for example.

On the other hand, in water and most other liquids the Prandtl number is large, so that viscosity becomes important at wave numbers where the thermal diffusivity does not yet affect the temperature spectrum. The range of wave numbers where $\kappa\eta \geqslant 1$, but $\kappa\eta_\theta \ll 1$, is called a *viscous-convective subrange.* Of course, there is also a range where $\kappa\eta \gg \kappa\eta_\theta \geqslant 1$; this is called the *viscous-diffusive subrange.*

The inertial-diffusive subrange In fluids with low Prandtl numbers, an inertial-diffusive subrange exists for $\kappa\eta_\theta \geqslant 1$, $\kappa\eta \ll 1$. In this range, the spectral flux of kinetic energy is constant and equal to ϵ. However, the spectral flux of temperature variance, which is equal to N in the inertial-convective subrange, decreases in the inertial diffusive subrange because of local dissipation of temperature variance:

$$dT_\theta/d\kappa = -2\gamma\kappa^2 E_\theta. \tag{8.6.15}$$

This equation can be solved only if we adopt the cascade model (8.6.11) of the spectral transfer T_θ. In the inertial-diffusive subrange, $E(\kappa) = \alpha\epsilon^{2/3}\kappa^{-5/3}$, so that (8.6.11) becomes

$$T_\theta = C\alpha^{1/2}\epsilon^{1/3}\kappa^{5/3}E_\theta. \tag{8.6.16}$$

Comparing this with (8.6.14), we find that (8.6.16) amounts to replacing N by T_θ in (8.6.14). Hence, we are using inertial scaling, as in (8.6.14), but based on the local value of T_θ. This can be a fair approximation only if T_θ changes slowly with wave number. The comparison of (8.6.14) and (8.6.16) also shows that we should take $C\alpha^{1/2} = \beta^{-1}$.

The solution of (8.6.15, 8.6.16), with $C\alpha^{1/2} = \beta^{-1}$, is (Corrsin, 1964)

$$E_\theta(\kappa) = \beta N\epsilon^{-1/3}\kappa^{-5/3}\exp[-\tfrac{3}{2}\beta(\kappa\eta_\theta)^{4/3}]. \tag{8.6.17}$$

Here, the temperature microscale η_θ is defined by

$$\eta_\theta \equiv (\gamma^3/\epsilon)^{1/4}. \tag{8.6.18}$$

This scale was discovered by Corrsin (1951). At present, no measurements exist with which (8.6.17) can be compared. The spectrum is well behaved at large wave numbers, but it cannot be valid far into the inertial-diffusive subrange because the assumptions on which it is based are not valid there.

Because (8.6.18) is identical in shape with (8.4.6), the peak in the spectrum of dissipation of temperature variance occurs at $\kappa\eta_\theta = 0.2$. Also, if we want to truncate the spectrum at the high wave-number end, we have to put the cutoff point at $\kappa\eta_\theta = 0.55$.

The viscous-convective subrange A viscous-convective subrange occurs at wave numbers such that $\kappa\eta \gg 1$, $\kappa\eta_\theta \ll 1$, in fluids with a large Prandtl number. In this range, the scales of temperature fluctuations are progressively reduced by the strain-rate field (see Sections 3.4 and 7.3), but the thermal diffusivity is not yet effective. Temperature fluctuations at wave numbers beyond $\kappa\eta = 1$ experience strain-rate fields of magnitude $(\epsilon/\nu)^{1/2}$ and size η. Because the energy spectrum drops off so sharply near $\kappa\eta = 1$, the extent of the strain-rate fields appears to be infinite to small temperature eddies at $\kappa\eta \gg 1$. Therefore, only $(\epsilon/\nu)^{1/2}$ should be important, but not η. In the viscous-convective subrange, we thus expect that $E_\theta = E_\theta(\kappa, N, (\epsilon/\nu)^{1/2})$.

This must have the form

$$E_\theta(\kappa) = cN(\nu/\epsilon)^{1/2}\kappa^{-1}. \tag{8.6.19}$$

This spectrum was first predicted by Batchelor (1959); measurements by Gibson and Schwartz (1963) have confirmed its existence. It should be noted that (8.6.19) can also be obtained (but less rigorously) from the "mixing-length" estimate (8.6.11) of the spectral transfer T_θ. This is done by replacing the strain rate $(\kappa^3 E)^{1/2}$ in (8.6.11) by $(\epsilon/\nu)^{1/2}$ and putting $T_\theta = N$, because the effects of γ are presumed to be small.

The viscous-diffusive subrange At very large wave numbers, molecular diffusion of temperature fluctuations becomes effective. The viscous-convective subrange ends when the scale of the temperature fluctuations has become so small that diffusion becomes significant for time scales of the order of the period $(\nu/\epsilon)^{1/2}$ of the strain-rate fluctuations. Diffusion spreads hot spots of size ℓ at a rate determined by $\ell^2 \sim \gamma t$; the smallest scale (η_θ) is obtained if t is replaced by $(\nu/\epsilon)^{1/2}$. This yields

$$\eta_\theta/\eta = (\gamma/\nu)^{1/2}. \tag{8.6.20}$$

This estimate, which is valid only for $\gamma/\nu \ll 1$, was obtained earlier in Sections 3.4 and 7.3.

The shape of the spectrum near $\kappa\eta_\theta = 1$ can be estimated in the now familiar way by adopting almost-inertial scaling for T_θ. As the viscous-diffusive subrange is approached, T_θ begins to decrease slowly. As long as T_θ is not too different from N, we may generalize (8.6.19) as

$$E_\theta(\kappa) = cT_\theta\ (\nu/\epsilon)^{1/2}\kappa^{-1}. \tag{8.6.21}$$

This states that T_θ is proportional to the amount of temperature variance in eddies of scale κ, which is κE_θ, and to the strain rate $(\epsilon/\nu)^{1/2}$. Substituting (8.6.21) into (8.6.15), we obtain

$$E_\theta(\kappa) = cN(\nu/\epsilon)^{1/2}\kappa^{-1}\exp[-c(\kappa\eta_\theta)^2], \tag{8.6.22}$$

in which η_θ is given by (8.6.20). The location of the exponential cutoff obtained this way agrees with the estimate (8.6.20). Again, although (8.6.22) is well behaved, it is certainly not valid for $\kappa\eta_\theta \gg 1$, because it is based on (8.6.21), which certainly is not valid there.

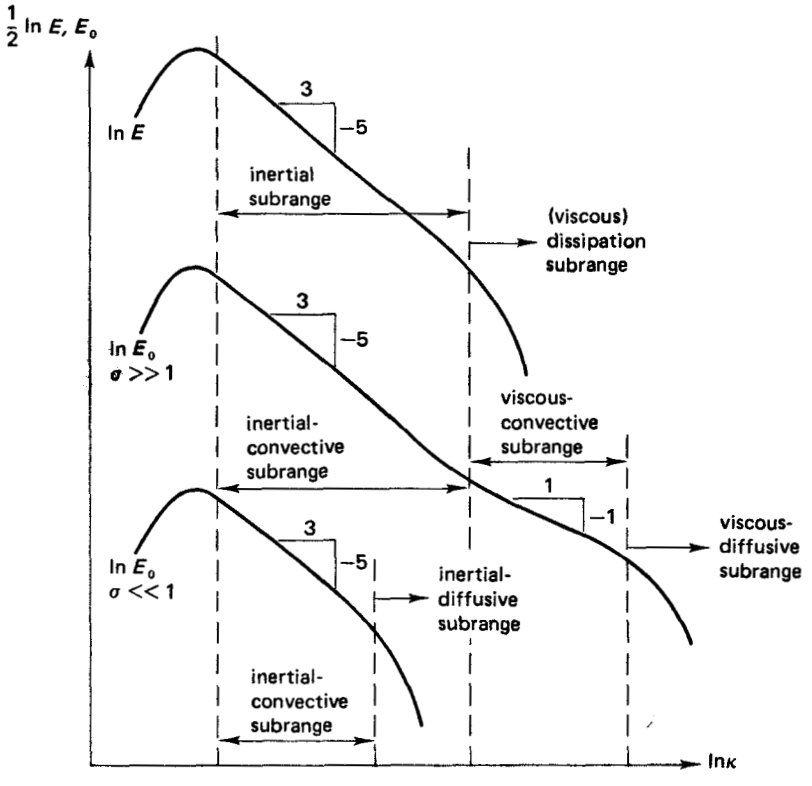

Figure 8.11. Spectra of temperature variance in liquids with large and small Prandtl numbers.

Summary The various subranges in the spectrum of temperature variance, for liquids with large and small Prandtl number, are sketched in Figure 8.11. The Reynolds number, of course, is assumed to be large.

Problems

8.1 What is the shape of the correlation function $\overline{u(x)u(x+r)}$ in a range of values of r which corresponds to the inertial subrange?

8.2 In the spectral energy transfer model of Corrsin, the energy transfer across given wave number is approximated by a mixing-length expression that is not corrected for viscous effects as $\kappa\eta = 1$ is approached. Make a similar

model for the momentum transfer in the inner layer of a turbulent boundary layer in zero pressure gradient. Integrate the resulting equation of motion and show that, unlike its spectral counterpart, this model does not give an accurate representation of the mean flow in the inner layer.

8.3 Derive expressions for the evolution of the kinetic energy and of the integral scale of isotropic turbulence in the initial period of decay (see Section 3.2). Do this by calculating the evolution of an approximate energy spectrum that consists of an inertial subrange at high wave numbers and a spectrum of the type $E(\kappa) \sim \kappa^4$ (8.1.16) at low wave numbers. Assume that the constant C in (8.1.16) is independent of time (this is called the "permanence of the largest eddies" (Batchelor, 1953)). Show that the Reynolds number of isotropic turbulence decreases in time during the initial period of decay, in contradiction with the result given in Section 3.2.

8.4 In the final period of decay of isotropic turbulence, the Reynolds number is so small that no energy exchange between wave numbers takes place. Calculate the rate of decay of the kinetic energy, assuming that the spectrum at the beginning of the final period of decay is given by (8.1.16), with C independent of time (see also Problem 8.3).

8.5 A small, heavy particle rapidly falls through a field of isotropic turbulence. Because the terminal velocity of the particle is large, its path is nearly straight, so that the particle, in first approximation, experiences a frequency spectrum corresponding to the one-dimensional Eulerian space spectrum. If the terminal velocity is V_T, the relation between frequency and wave number is $\omega = \kappa V_T$. Under certain conditions, the equation for the horizontal particle velocity v may be approximated by $T\,dv/dt + v = u$, where $T = V_T/g$ is the particle time constant and u is the horizontal fluid velocity experienced by the particle. Calculate the horizontal dispersion of the particle and compare it with the Lagrangian dispersion experienced by a particle with vanishingly small V_T.